Effect of Physical Properties of Synthesized Protic Ionic Liquid On Carbon Dioxide Absorption Rate

Amita Chaudhary (amita.chaudhary@nirmauni.ac.in)
Nirma University Institute of Technology https://orcid.org/0000-0002-4699-0375
Ashok N Bhaskarwar
Indian Institute of Technology Delhi

Research Article

Keywords: Protic Ionic Liquids (PILs), Gas-Liquid Interface, NMR, FTIR, Carbon-dioxide Absorption, Stirred-Cell Reactor, Kinetic Studies

Posted Date: September 20th, 2021

DOI: https://doi.org/10.21203/rs.3.rs-857017/v1

Version of Record: A version of this preprint was published at Environmental Science and Pollution Research on January 8th, 2022. See the published version at https://doi.org/10.1007/s11356-021-17154-6.

Effect of Physical Properties of Synthesized Protic Ionic Liquid on Carbon dioxide Absorption Rate

Amita Chaudhary[1,*] and Ashok N Bhaskarwar[2]
[1]Department of Chemical Engineering, Nirma University, Ahmedabad, Gujarat, INDIA.
[2]Department of Chemical Engineering, Indian Institute of Technology Delhi, Hauz Khas, New Delhi, INDIA.
[*]Corresponding Author mail.id: amita.chaudhary@nirmauni.ac.in
Ph. 91-011-26591028(O)

Abstract

Concentration of carbon dioxide gas has accelerated from the last two decades which cause drastic changes in the climatic conditions. In industries, carbon capture plants use volatile organic solvent which causes many environmental threats. So, a low-cost green absorbent has been formulated with nontoxicity and high selectivity properties for absorbing carbon dioxide gas. This paper contains the synthesis process along with the structure confirmation using ^{1}H NMR, ^{13}C NMR, FT-IR, and mass spectroscopy. Density, viscosity, and diffusivity are measured at different ranges with standard instruments. The kinetic studies were also conducted in a standard predefined-interface stirred-cell reactor. The kinetic parameters were calculated at different parameters like agitation speeds, absorption temperature, initial concentrations of ionic liquid, and partial pressure of carbon dioxide. The reaction regime of carbon dioxide absorption is found to be in fast reaction kinetics with pseudo first order. The reaction rate and the activation energy of CO_2 absorption are experimentally determined in the range of 299 K to 333K with different initial concentrations of ionic liquid (0.1-1.1 kmol/m^3). The second order rate constant and activation energy of carbon dioxide absorption in the synthesized ionic liquid is found to be (6385.93 to 12632.01 m^3 mol-1 s-1) and 16.61 kJ mol^{-1} respectively. This solvent has shown great potential to absorb CO_2 at large scale.

Keywords: Protic Ionic Liquids (PILs); Gas-Liquid Interface; NMR; FTIR; Carbon-dioxide Absorption; Stirred-Cell Reactor; Kinetic Studies.

25 **Abbreviations**

A	Arrhenius Pre-exponential factor, m^3/mol s
a	volumetric Gas-Liquid Interfacial Area, m^{-1}
B	base (water)
C_A	the concentration of species A in the liquid phase in the foam film, k mol/m^3
C_B	the concentration of reactant B in the liquid phase in the storage section at time t, k mol/m^3
C_{B0}	the initial concentration of reactant B in the liquid stream entering the storage section, k mol/m^3
C_{TETAL}	initial Concentration of [TETA] [Lactate], k mol/m^3
CO_2	Carbon-dioxide gas
$C_{2,i}$	CO_2 concentration at G-L interface, mol/m^3
D_A	the diffusion coefficient of reactant A in the liquid phase, m^2/s
D_{CO_2}	diffusion coefficient of carbon dioxide in the [TETA] [Lactate] solution, m^2 /s
$D_{CO_2}^{H_2O}$	diffusivity of CO_2 in water, m^2/s
D_S	the diameter of impeller blades in the liquid-phase, m
$D_{Stirred-cell}$	the inner diameter of stirred tank reactor, m
E_a	Activation energy, kJ/mol
E_A	enhancement Factor
E_i	instantaneous enhancement factor
G-L	Gas-Liquid Interface
H_{CO_2}	Henry's constant for carbon-dioxide on [TETA] [Lactate] solution
Ha	Hatta Number
ILs	ionic Liquids
$k_l{}^a$	volumetric mass transfer coefficient, m/s
k_{-1}	the backward first-order reaction rate constant, s
k_2	the forward second-order reaction rate constant for the formation of the zwitterion, m^3/mol. s
k_{ov}	overall pseudo-first order reaction rate constant, s^{-1}
k_B	Rate constant for the deprotonation of the zwitterion by a base, m^3/ mol. s
n	number of moles, k mol

26

1. Introduction

Carbon dioxide (CO_2) levels rose by 2.6 ppm in 2019, faster than the average rate for the last ten years, which was 2.37 ppm. This has drawn a concerned mark globally. The major sectors responsible for CO_2 emission are manufacturing industries and fossil-fuel based industries (Li *et al.*, 2019). So, there is a high demand of improving the existing mitigation methods for minimising the CO_2 level in the atmosphere. Currently, in absorption technology, CO_2 gas is scrubbing using alkanolamines. Among alkanolamines, monoethanolamine (MEA), diethanolamine (DEA), and methyl diethanolamine (MDEA) along with some promoters are widely used. Research is ongoing to find new and eco-friendly solvent having high selectivity and absorption capacity for carbon dioxide that react faster and require less energy to regenerate in comparison to the existing solvents (Liu *et al.*, 2018). The rate of CO_2 absorption and regeneration rate of CO_2 –rich solvent depends upon their chemical composition and thermo physical properties. The biggest limitation with the protic ionic liquids are their continuous increase in viscosity on absorbing carbon dioxide due to the formation of carbamate. So, this article covers the development of ionic liquid from amine, their structure elucidation using ^{1}H NMR, ^{13}C NMR, FTIR, and mass Spectroscopy. The effect of density and viscosity on the rate of CO_2 absorption also investigated experimentally. In earlier publications, limited reaction kinetics of CO_2 in protic ionic liquids are available. They concluded that these ionic liquids reacted rapidly with CO_2 and were capable of absorbing a high quantity of CO_2 stoichiometrically. This article also contains the detailed kinetic studies of CO_2 absorption in stirred cell reactors. The stirred-cell reactor is a stirred vessel with an undisturbed (flat) gas-liquid interface and both the phases are stirred separately. Due to which the k_L $(liquid - side\ mass\ transfer\ coefficient)$value decreases in comparison to the other reactors like bubble column, jet reactor, etc. For fluids like water and gases like CO_2, O_2 the k_L values are lying in the range of $2\text{-}15\times10^{-3}$ cm/sec (Gates 1985). For kinetic studies in gas-liquid reactions, stirred cell contactor is probably the most versatile reactor to employ at the lab scale. Many gas absorption studies have been taken in the stirred cells operated at the speed of 20-150 rpm without significant vortex formation. Sauchel and group studied the absorption of ammonia in aqueous acid solution for the manufacture of nitrogenous fertilizers(Sauchel 1960). In 1964, Sharma reported CO_2-absorption in carbonate buffers with or without a catalyst(Sharma 1964). The absorption studies of oxygen in aqueous sodium sulfite(Linek 1966). Gupta and Sharma, 1967, worked on CO_2-absorption in barium sulphide(Gupta and Sharma 1967). Miller, 1969, examined the absorption of C_2H_4 in ethylene dibromide(Miller 1969). Chaudhari and Doraiswamy, 1974, used mechanically agitated contactor for absorption of phosphine in aqueous solutions of formaldehyde and HCl(Chaudhari and Doraiswamy 1974). Sridharan and Sharma (1976) studied the carbon-dioxide absorption rate in amines and

alkanolamines dissolved in organic solvents such as isopropanol, n-butanol, cyclohexanol, aqueous diethylene glycol, toluene, and o-xylene in the stirred contactor. Oyevaar and Westerterp, 1989, investigated solubility of phosphine in aqueous solutions of sodium hypochlorite and sulfuric acid (Oyevaar and Westerterp 1989). Lahiri et al., 1981, did experimental studies on the dissolution of NO in aqueous solutions of alkaline sodium dithionite(Lahiri, Yadav, and Sharma 1981). Kucka et al., 2003, studied the absorption of CO_2 in MEA solution in a stirred cell(Kucka et al. 2003). Jean-Mare et al., 2009, investigated the CO_2-absorption in the mixture of N-methyl diethanolamine and triethylenetetramine(Jean-Mare, Amann, and Bouallou 2009). Zhou et al., 2012, analyzed the CO_2-absorption kinetics in tetramethylammonium glycinate [N_{1111}] [Gly] and 2-amino-2-methyl-1-propanol solution(Stevanovic et al. 2013). Ying and Eimer, 2013, performed a kinetic study of CO_2-absorption in aqueous MEA solution at different temperatures and concentrations of MEA(Ying and Eimer 2013). Iliuta et al., 2014, worked out CO_2-absorption in diethanolamine/ionic liquid emulsions(Ying and Eimer 2013). All these studies were performed in a stirred tank reactor. Some of the activation energies of CO_2 absorption with the stirred cell reactor at ambient condition are tabulated in Table 1.

Table 1: Activation energy of the systems studied for CO_2 absorption

CO_2 Capturing system	**Activation energy ($kJ\ mol^{-1}$)**	**References**
Hexamethylenediamine (HMDA) and sodium glycinate (SG)	10.76	(Mondal and Samanta, 2020)
BZA–H_2O–CO_2	25.6	(Mukherjee, Bandyopadhyay and Samanta, 2018)
MDEA and [C_2OHmim][Gly]	11.24	(Sun *et al.*, 2017)
[N_{1111}] [Gly] and 2-amino-2-methyl-1-propanol	13.4	(Zhou, Jing and Zhou, 2012)
AMP and [Hmim][Gly]	8.08	(Zhou *et al.*, 2016)
MEA and [Bmim][NO_3]	11.25	(Zhang *et al.*, 2014)
MDEA and [Bmim][BF_4]	9.06	(Ahmady, Hashim and Aroua, 2012)
MEA and [Bmim][BF_4]	10.04	(Lu *et al.*, 2013)
[P_{66614}][pro] and tetraglyme	43	(Gurkan *et al.*, 2013)
[P_{66614}][2-CNpyr] and tetraglyme	18	(Gurkan *et al.*, 2013)
[TETA] [Lactate]+H_2O	16.61	This work

1.1 Proposed Reaction Mechanisms

The chemical absorption reactions of carbon-dioxide with primary and secondary amines are identified well in literature initially by Caplow (1968) followed by Danckwerts (1979) (Sun *et al.*, 2017). This mechanism involves two steps:

(I) First Step: formation of the CO_2-amine complex (Caplow, 1968). It includes two steps.

(i) Formation of zwitterion intermediate complex:

$$CO_2 + R_1R_2NH \quad R_1R_2N^+HCOO^- \qquad \ldots (1)$$

(ii) De-protonation of the zwitterion (Danckwerts, 1979):

$$R_1R_2N^+HCOO^- + :B \;\; k_B \rightarrow \; R_1R_2NCOO^- + \; BH \qquad \ldots (2)$$

(II) Second Step: Ter-molecular mechanism (Crooks & Donnellan and Alper, 1989) (Thummuru and Mallik, 2017).

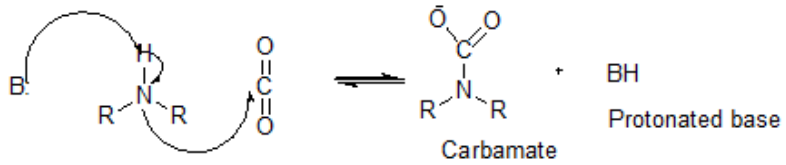

…(3)

Theoretically, one mole of carbon-dioxide gas reacts with two moles of amines, i.e. 0.5 moles of CO_2 react per mole of amine, whereas in case of a tertiary amine absorb CO_2 in 1:1 mole ratio (Lee *et al.*, 2007). In this research, the synthesized ionic liquid is composed of four amine groups, having two primary amines and two are secondary amines. As per the basicity rule, the secondary amines are more basic and have higher affinity towards CO_2 than the primary amines, so the reaction takes place initially at secondary amine.

2. Experimental Work

2.1. Chemicals and Methodology

All chemicals and gases specified in Table 2, were used as purchased, no further purification was carried.

Table 2: CAS Reg. No Suppliers, Mass Fraction purity Molecular weight and Molecular formula of the chemicals used

Chemical	CAS Reg. No.	Suppliers	Mass fraction Purity	Molecular Weight and Molecular formula

Triethylene Tetramine	112-24-3	Central Drug House (P) Ltd New Delhi	0.89	146.24 g/mol, $C_6H_{18}N_4$
Lactic acid	79-33-4	Loba chemie	0.88	90.08 g/mol, $C_3H_6O_3$
Hydrochloric acid	7647-01-0	Sigma Aldrich	0.36 to 0.38	36.46 g/mol, HCl
Methyl Orange Indicator	547-58-0	Sigma Aldrich	0.85	327.33 g/mol $C_{14}H_{14}N_3NaO_3S$
CO_2 Gas Cylinder	-	Local gas vendor	0.99	44 g/mol , CO_2
N_2 Gas Cylinder	-	Local Gas Vendor	0.99	28 g/mol , N_2

Purity of gases was checked by ULTIMA-2100 series gas chromatograph of Nettle make. All solutions were prepared using de-ionised water in volumetric glassware.

2.2. Synthesis of Ionic Liquid

Equi-molar quantities of triethylenetetramine and lactic acid were taken in a three –necked round bottom flask equipped with a reflux condenser, a pressure funnel, and a mechanical stirrer. Initially, triethylenetetramine was taken in the round bottom flask and then lactic acid added drop by drop using a pressure funnel with constant stirring at 120 rpm using the mechanical stirrer. As the neutralization reaction produces a lot of heat, which is equal to -9 kcal/ mol, the round bottom flask was kept in an ice-water mixture. To avoid any contamination with air, the reaction mixture was placed under the N2 atmosphere. It was then stirred for several hours at room temperature. The completion of the reaction was monitored by TLC. The product was a pale yellow viscous liquid. Product was then washed with dichloromethane 2-3 times to remove impurities. Residual water is removed by vacuum heating at 80 ^{0}C for 12 hours. The ionic liquid was finally stored-in an airtight flask. The water content of the ionic liquid was analysed using the TGA analysis and found to be 0.01% (w/w).

2.3. Saturation studies of Carbon dioxide absorption

In all absorption experiments, pure carbon- dioxide gas is used. The gas was pre dried using infrared lamps and passed through a packed bed of 3 A˚ molecular sieves. The flow rate was 0.002 m^3 min^{-1}. Experiments were conducted in a round bottom glass reactor with an effective volume of 500 cm^3. The equilibrium study of carbon dioxide absorption was conducted in a 0.7 M solution of the ionic liquid at a temperature of 298.15 K and 1 atm for 70 hours. The reactor was loaded with approximately 300 cm^3 of the 0.7 M ionic-liquid solution. The reactor was then sparged with nitrogen to remove all the air impurities present above the interface of the solution before

each experiment. The vapour pressure of the ionic-liquid and solvent in the gas phase of the reactor was assumed to be constant, and equal to the total equilibrium pressure before the introduction of solute gas carbon dioxide to the reactor. Carbon dioxide was introduced into the reactor via mass flow controller (MFC) and a carbon dioxide rota-meter. Absorption reached a thermodynamic equilibrium after a sufficient time period, corresponding to the solubility limit of the gas in the ionic liquid at that temperature. Sample about 1ml of the reaction mixture were taken out at regular intervals of 5 minutes and weighed. The samples were then titrated with 2M HCl solution to analyse the carbon dioxide loading at a regular interval. The experimental setup is depicted in Figure 1.

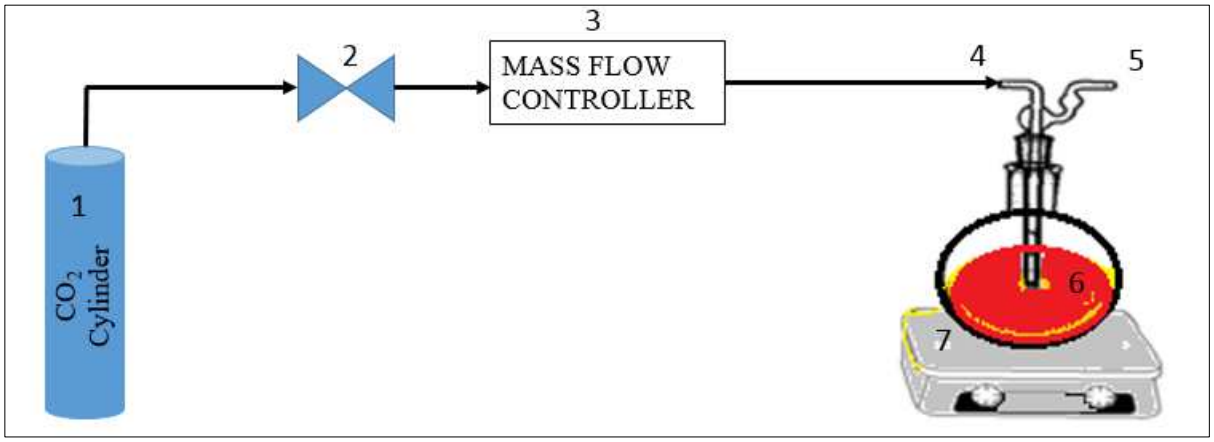

Figure 1. Experimental setup for CO_2 absorption. 1. CO_2 cylinder, 2. CO_2 rotameter, 3. Mass Flow Controller, 4. Gas inlet port, 5. Gas outlet port, 6. 0.7 M Ionic liquid solution, 7. Magnetic stirrer.

The amount of carbon dioxide absorbed in the ionic liquid solution was calculated by the following equation by assuming ideal gas behaviour:

Moles of CO_2 absorbed (α) =

$$\frac{(760\ mmHg - vapour\ pressure\ of\ water\ at\ ambient\ condition\ in\ mmHg)(Volume\ of\ displaced\ fluid - Volume\ of\ 2M\ HCl)}{(wt.of\ CO2\ rich\ sample \times R \times T \times 1000)} \quad \ldots(4)$$

2.4. Determination of physical properties of ionic liquids

The physical properties of the pure ionic liquid have a significant impact on gas-liquid reactions (Chen *et al.*, 2020). The viscosity, density, diffusivity, and Henry constant of the synthesized ionic liquid plays an important role in the diffusion process due to which the absorption rate of the carbon dioxide is affected (Littel, Versteeg, and Van Swaaij, 1992). These properties are determined using the standard instruments experimentally and theoretically both.

2.4.1. Viscosity

The dynamic viscosity of the pure ionic liquid was measured at different temperatures from 273 to 388 K using a Rheometer (Make: Anton Paar, Model: MCR302 SN81193479). Watanabe et al. (Tsuzuki et al., 2009) reported that the three main factors for the high viscosity of ionic liquids are due to its size, shape, and interaction between the anion and the cation. The interaction forces between anion and cation are coulombic forces, van der Waals forces, and hydrogen-bonding. Out of these forces, the coulombic forces are responsible and in carbon di-oxide absorbed ionic liquid hydrogen-bonding mainly cause viscosity. The viscosity of ionic liquid limited the diffusivity of the gas molecule in the ionic liquid.

2.4.2. Density

The density of synthesized ionic liquid was measured from 293 to 363 K using a densitometer (Make: DE45, Model: Mettler Toledo). The density of ionic liquid depends on the length of the alkyl chain. With each increase in $-CH_2$ group, the density of ionic liquid decreases which increases the free volume or sites available for CO_2 interaction.

2.4.3. Diffusivity D_{CO_2}

The rate of diffusion plays a significant role in the rate of absorption of a gas in liquid. So, the diffusivity of CO_2 has been determined using the Stokes-Einstein equation at various temperatures in the reactive solution.

I. Diffusivity of CO_2 in water is given by

$$D_{CO_2}^{H_2O} = 2.35 \times 10^{-6} exp(-\frac{2119}{T}) \text{ m}^2\text{s}^{-1} \quad \ldots(5)$$

II. Diffusivity of CO_2 in aqueous amine was considered the same for amine-based ionic liquids. (Versteeg and Van Swaaij, 1988)

$$D_{CO_2}^{aqu.amine} = D_{CO_2}^{H_2O} (\frac{\mu_{H_2O}}{\mu_{aqu.amine}})^{0.8} \text{ m}^2\text{s}^{-1} \quad \ldots(6)$$

2.4.4. Henry's law constant (H_{CO_2})

The solubility of a gas depends on the pressure exerted by a gas on the liquid surface. The pressure is different at different temperatures. So, it is also an important parameter in CO_2 absorption.

The values of Henry's law constant for the CO_2-H_2O system at different temperatures were obtained from Sander, R. (2015) (Sander, 2015)

$$H_{CO_2} = 3.03 \times 10^3 exp[-2400 \left(\frac{1}{T} - \frac{1}{298.15}\right)] \text{ mol m}^{-3} \text{ Pa}^{-1} \quad \ldots(7)$$

166 2.5. Kinetic Studies

167 **2.5.1. Stirred-cell reactor**

168 In gas-liquid absorption systems, semi-batch and counter-current contacting schemes predominate for better
169 efficiency and absorption (Levenspiel, 1999). A double jacketed stirred-cell reactor was used for the determination
170 of the kinetics of CO_2-absorption in ionic liquid solutions. A schematic representation of the stirred-cell reactor,
171 dimensions of the reactor and its internals are shown in fig. 1 and table 3.

172 Table 3. Dimensions of the Stirred-cell Contactor and its elements

Element	Dimension/Measurement
Volume of the reactor	1.33×10^{-3} m^3
Total length	0.2 m
Inner diameter	0.105 m
Diameter of gas-side impeller blades	0.056 m
Diameter of liquid-side impeller blades	0.05 m
Number of baffles	4
Liquid-phase volume	0.5×10^{-3} m^3
Cross-sectional / gas-liquid interface area	8.65×10^{-3} m^2

173

174

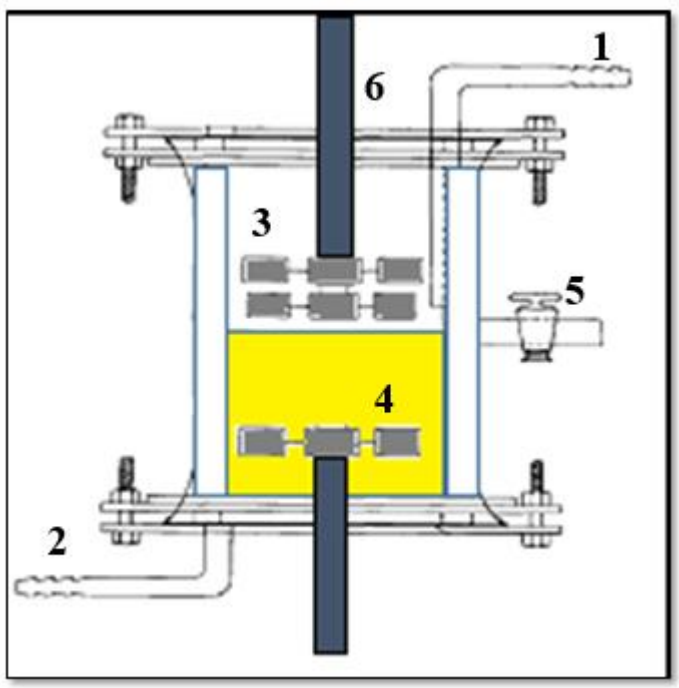

175

176 Figure 2. Schematic representation of Stirred-cell Contactor (adapted from Doraiswamy and Sharma (1984) (1.
177 Gas-outlet port, 2. Gas-inlet port, 3. Gas-side impeller, 4. Liquid-side impeller, 5. Liquid sample port, 6.Shaft).

Both phases were stirred separately using the different impellers to minimize the mass transfer resistance. A pair of 6-bladed-disk-turbine impellers and 4-bladed-disk-turbine impellers of stainless steel were used in gas phase and liquid phase simultaneously. These impellers were mounted on a standard shaft. Digital temperature sensors (PT100) and pressure gauge were provided to monitor the temperature and pressure in real time for measuring CO_2-absorption. The temperature inside the reactor was maintained constant to within ± 0.1 °C using a double jacket in which water is circulated continuously. A vacuum pump is also equipped with the gas-outlet port to remove the gases and volatile impurities from the reactor at the beginning and end of the absorption experiments.

2.5.2. Methodology

All experiments were conducted in the above-mentioned reactor in a semi-batch mode with the 0.5 M aqueous solution of synthesised ionic liquid. The ionic liquid solution is charged in/as a batch, and pure CO_2 gas is passed continuously through it from the bottom in a semi-batch mode of process. The CO_2-absorption experiment begins with the sparging of N_2 gas into the reactor at 2 LPM for 15 minutes to eliminate all residues of CO_2 or all the gaseous impurities present. Leakages of gas and liquid from the experimental setup were also tested prior to the conduction of experiments using soap solution. A calibrated rota-meter was used to measure the CO_2 flow rate, accompanied by a digital mass-flow controller (MFC). Initially, 500 mL of an aqueous solution of ionic liquid was charged into the reactor and then pure CO_2 gas was introduced in it through the gas inlet- port. During the experiment, both phases were stirred constantly and individually. At the beginning and end of the experiment, temperature and pH of the liquid-phase were recorded using the pre-calibrated fitted instruments. After a specific period, 1mL of the reacted solution was sampled and tested by the Chittick apparatus (Crossno, Kalbus and Kalbus, 1996) for calculating CO_2 gas loading. In-flow of the CO_2 reactor and the agitation were stopped at the time the sample was drawn. The absorption runs were repeated for different times until the ionic liquid solution got saturated with CO_2 gas. The absorption experiments are also conducted using the same method and by varying the different parameters. Arrhenius plot is also made by conducting the absorption studies at different temperatures and activation energy of CO_2 absorption were calculated.

2.5.3. Equations and reactions involved

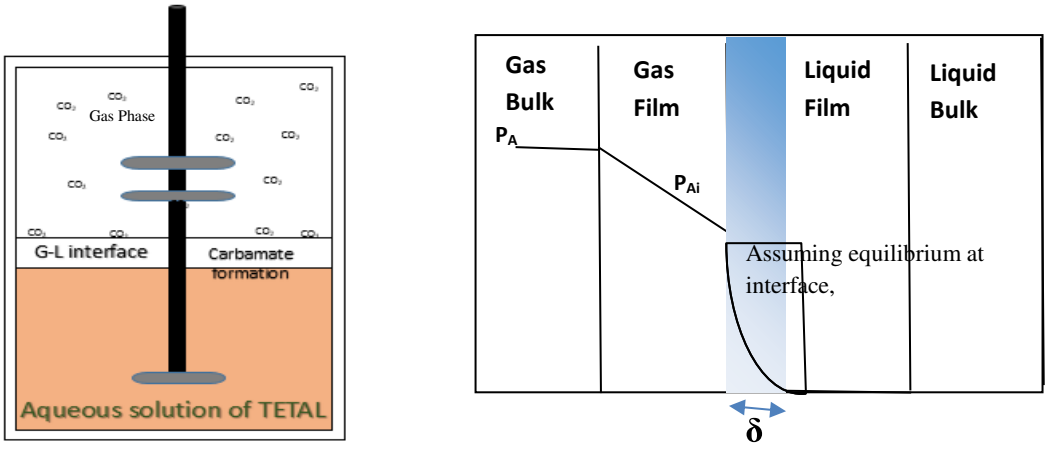

(a) (b)

Figure 3. Schematic representations of (a) Stirred- cell contactor with flat interface, and (b) Partial-pressure and concentration profiles of CO_2 in the gas phase and liquid phase, respectively during the diffusion and chemical reaction of CO_2 in ionic liquid (fast –reaction regime)

The gas-absorption system, i.e. a stirred-cell contactor chosen is shown schematically in fig. 3, illustrates the concentration profiles of carbon dioxide in gas-phase bulk, in gas film, and in the film and in the bulk liquid.

Let us assumed that CO_2 gas absorption in ionic liquid solution is an irreversible second order reaction and can be represented as:

General equation for second-order reaction,

$$A_g + nB_l \longleftrightarrow P_l \qquad \ldots (8)$$

Here, A represents the CO_2 gas, B represents ionic liquid, and P is the liquid product formed after the chemical absorption reaction between A and B. For our system, the above equation can be modified as,

$$CO_2(g) + zTETAL(l) \rightarrow P(\text{carbamate})(l) \qquad \ldots (9)$$

Consider the following cases of absorption as,

Case 1: When the carbon dioxide reacts entirely in the gas-liquid interface film with film thickness (δ), the enhancement factor is calculated from the following expression (Dudukovic, 1986)

$$E_A = \frac{J_{CO2}a}{k_L.C^*_{CO2}.a} = \frac{1}{k_La}.\frac{k_H}{V_{aqu.TETAL}}.\frac{V_{CO_2}}{P_{CO_2}.R.T}\left(\frac{dP_{CO_2}}{dt}\right) \qquad \ldots (10)$$

$$Ha = \frac{\sqrt{\frac{2}{m+1}D_{CO_2}k_{mn}(C^*_{CO_2})^{m-1}C^n_{TETAL}}}{k_L} \gg 1 \qquad \ldots (11)$$

Case 2: When there is no change in the concentration of ionic liquid in the liquid film, the following condition will be satisfied

$$\text{Ha} = \frac{\sqrt{\frac{2}{m+1} D_{CO_2} k_{mn} (C^*_{CO_2})^{m-1} C^n_{TETAL}}}{k_L} \ll \frac{C_{TETAL}}{Z C^*_{CO_2}} \sqrt{\frac{D_{TETAL}}{D_{CO_2}}} \quad \ldots (12)$$

The enhancement factor, E, is a function of the Hatta number (Ha) and the instantaneous enhancement factor (E_i) defined as

$$E_i = \sqrt{\frac{D_{CO_2}}{D_{TETAL}}} + \frac{C_{TETAL}}{Z C^*_{CO_2}} \sqrt{\frac{D_{TETAL}}{D_{CO_2}}} \quad \ldots (13)$$

$$E = -\frac{Ha^2}{2(E_i - 1)} + \sqrt{\frac{Ha^4}{4.(E_i - 1)^2} + \frac{E_i . Ha^2}{(E_i - 1)} + 1} \quad \ldots (14)$$

Case 3: For the fast pseudo-first order reaction regime, the following conditions should be satisfied, Ha > 2, E_i / H_a > 5, $H_a \approx E$, and H_a and k_{ov} are related by

$$Ha = \frac{\sqrt{D_{CO_2} k_{ov}}}{k_L} \text{ , or } \ldots (15)$$

$$k_{ov} = \frac{(H_a . k_L)^2}{D_{CO_2}} \quad \ldots (16)$$

The second-order forward reaction-rate constant, k_2 , can therefore be calculated from

$$k_2 = \frac{(N_{CO_2})^2}{(C^*_{CO_2})^2 . D_{CO_2} . C_{TETAL}} \quad \ldots (17)$$

The governing differential equation for the diffusion and chemical reaction of carbon dioxide in the film can thus be written as

$$D_{CO_2} \frac{d^2 C_{CO_2}}{dx^2} = k_{mn} . C^m_{CO_2} . C^n_{TETAL} \quad \ldots (18)$$

$$= k_m . C^m_{CO_2} \quad \ldots (19)$$

, Where
$k_m = k_{mn} . C^n_{TETAL}$,
and the concentration of the ionic liquid in the solution remains constant throughout the film.

Then, the specific rate of CO_2 absorption can be calculated as,

$$R_{CO_2} = C^*_{CO_2} . \sqrt{\frac{2}{m+1} D_{CO_2} k_{mn} (C^*_{CO_2})^{m-1} . C^n_{TETAL_0}} \quad \ldots (20)$$

The rate of transfer of CO_2 from gas to liquid phase can be expressed by the rate expression for liquid film by

$$R_{CO_2}(t) = k_L a \left({C_{CO_2}}^* - {C_{CO_2}}^{bulk} \right) \quad \ldots (21)$$

The second-order reaction rate constant, k_2, may then be obtained using equation (20).

3. Results and discussion

3.1. Characterization of synthesized ionic liquid

The photograph of synthesized ionic liquid shown in fig.4 is a pale-yellow oily appearance liquid. The structure of ionic liquid was confirmed using various instrumental techniques, viz. FT-IR, ^{1}H NMR, ^{13}C NMR, and Mass spectroscopy. The structure of prepared ionic liquid is shown in table 4.

Table 4. Proposed structure of ionic liquid with IUPAC nomenclature

Ionic Liquid	Common Name	IUPAC Nomenclature
TETAL	triethylene tetra ammonium Lactate	{2-[(2-aminoethyl)amino]ethyl}(2-azaniumylmethyl) amine 2-hydroxypropanoate

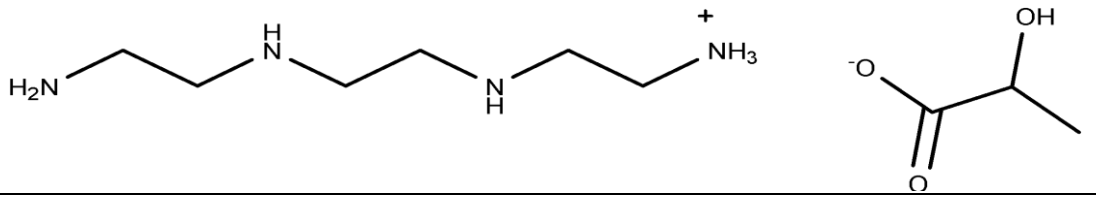

Figure 4. Photograph of synthesized ionic liquid

The prepared ionic liquid is the result of transformation of triethylenetetramine (TETA) to triethylenetetrammonium ($TETA^{+}$) cation and Lactate anion from Lactic acid.

3.1.1. FT-IR data

The IR spectrum of ionic liquid (TETAL) was done using the PerkinElmer infrared spectrophotometer and results are explained using fig.5 and table 5. A Perkin Elmer Spectrum 400 FTIR/FT-NIR Spectrometer was used to analyse both the LDPE and PS dissolving product samples (Perkin Elmer, New Delhi). For analysis, a small layer of sample is put between two KBr pallets. Before testing, KBR powder was finely powdered with a mortar and pestle and dried in a vacuum oven at 60 ^{o}C before being formed into pellets with a thickness of 0.8 mm. The

wavelength range of 4000–650 cm^{-1} was used to obtain infrared spectra. Before comparison with standard spectrum, all spectra were baseline corrected and normalised using the spectrum in-built feature.

Table 5. FT-IR of ionic liquid with its molecular vibrations at different wavelength

Type of molecular vibrations	Wave number (cm^{-1})
N-H stretching,(-NH_2)	3390.49 and 3291.22
N-H stretching,(-NH)	3354.69
N-H bending	1597.02
C–N stretching (aliphatic amines)	1141.06-1116.18
N-H wagging	973.67-732.96
NH_3^+ bending	1451.57
N-CH_2	2789.61 - 2809.79
-CH_2 (Aliphatic methylene chain)	2842.76 - 2933.06

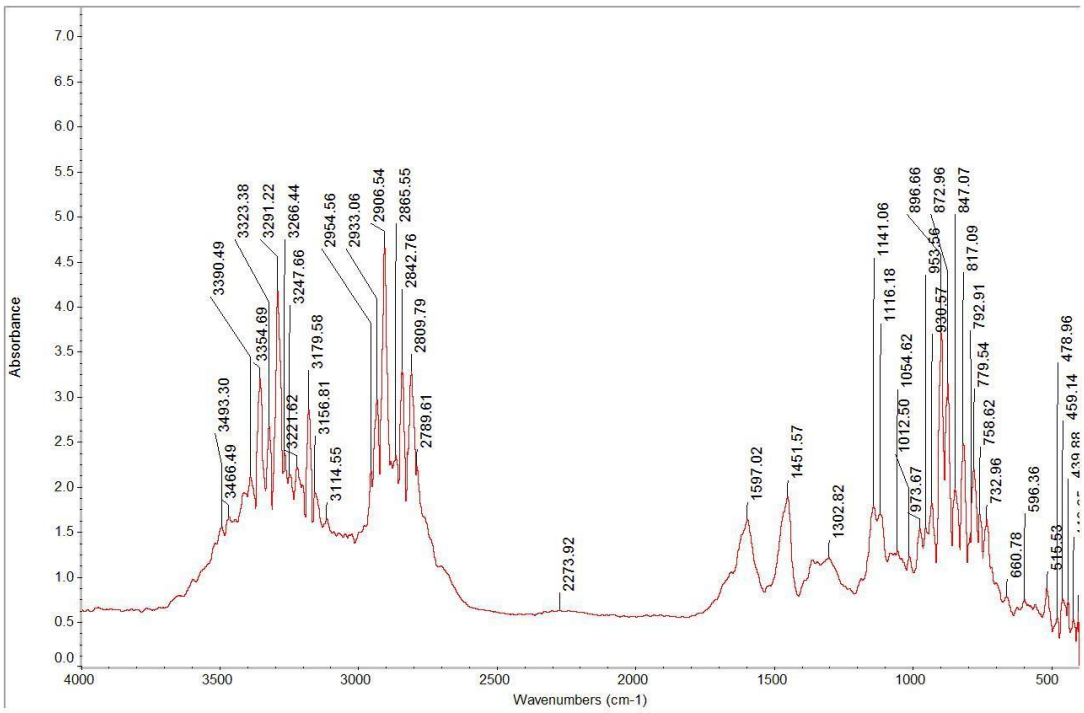

Figure 5. FT-IR of synthesized ionic liquid

From FTIR studies, it is revealed that the given synthesised molecule contains both primary and secondary amine basic sites. The presence of basic sites make it suitable for absorbing acidic gases. The molecule is showing multiple strong bands in the range of 2789.61-2809.79 and 2842.76 – 2933.06 for aliphatic amines (–N-CH_2) and aliphatic alkyl chain.

3.1.2. NMR

Two types of NMR were done: proton NMR (^{1}H-NMR) and carbon-13 (^{13}C-NMR) to check the position and environment of different hydrogen atoms and carbon atoms in the molecular structure of ionic liquid. The characterization was done using a Bruker 300 MHz spectrometer having N_2 as carrier gas. A sample was prepared in deuterated DMSO-d_6. To eliminate the noise disturbance between the DMSO-d_6 and the ionic liquid, a separate capillary tube was used for loading DMSO-d_6 with the ionic liquid in the NMR tube.

^{1}H-NMR

The residual proton in DMSO-d6 appeared at 2.50 ppm set as the ^{1}H NMR external reference. The positions and environment of different hydrogen atoms or protons present in ionic liquid is shown in Figure 6.

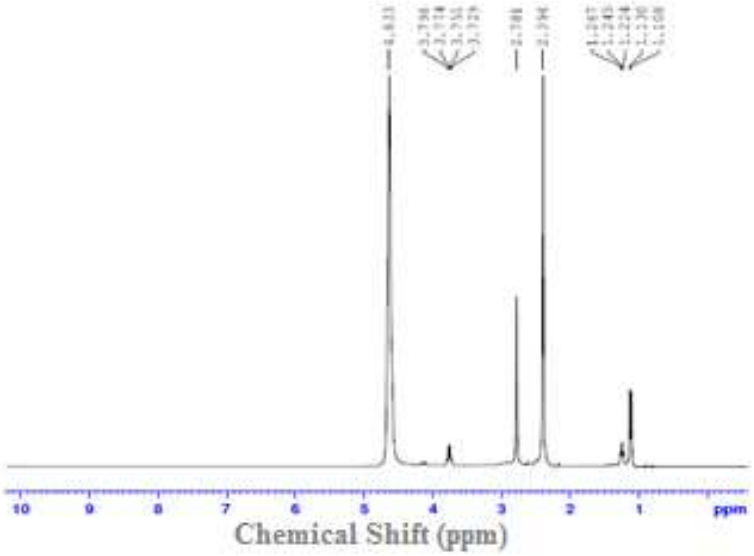

Figure 6. ^{1}H NMR of synthesized Ionic liquid

Table 6. ^{1}H-NMR of synthesized ionic liquid

Chemical Shift (ppm)	Proton Environment
1.119	(small)- 3H, CH_3, DMSO-d_6
2.347, 2.724, 2.593	CH_2N
4.4	(broad and small)- NH, NH_2

The proton NMR of synthesised ionic liquid shows the characteristic chemical shifts which helps in confirming the structure of ionic liquid. The chemical shift at 2.34-2.72 ppm represents the protons associated with carbon and nitrogen in the structure. The broad and small peaks visible at 4.4 ppm denotes the protons associated with primary and secondary amines.

330 **^{13}C-NMR**

331 ^{13}C NMR spectra of ionic liquid was also obtained using Bruker 300 MHz spectrometer having N_2 as carrier gas
332 to finalize the position of different carbon atoms present in the ionic liquid. The different chemical shifts for
333 various types of carbon present in DMSO-d_6 and ionic liquid are discussed below in table 7.

334

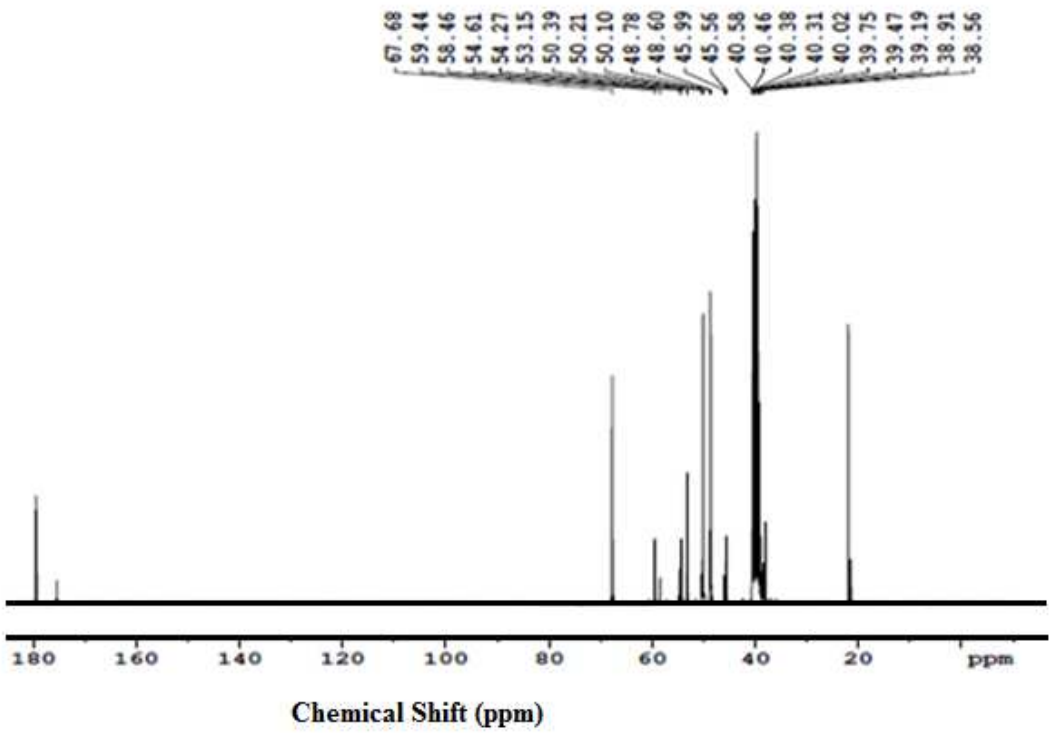

335

336 **Figure 7. ^{13}C NMR of Synthesized ionic liquid**

337 Fig.7 contains the ^{13}C Chemical Shifts of the ionic liquid cation relative to trimethylsilane (TMS). The ^{13}C
338 Chemical Shifts at 40,45, and 50 ppm shows the presence of carbon atoms in the environment of primary and
339 secondary amines respectively. The characteristic peak at 179.38 is the confirmed peak of the carboxyl group
340 present in the lactate ion. The carbon associated with the -OH group in lactate ion is shown at 67.38 ppm.

341 **Table 7. ^{13}C NMR of synthesized ionic liquid**

Chemical Shift (ppm)	Type of C-atom
39.5	DMSO-d_6, reference peak
40	- CH_2N
45	-CNH_2

50	-CNH
67.68	-CHOH
179.38	-COOH

3.1.3. Mass Analysis

The mass analysis of ionic liquid is done using a mass spectrometer with cation and anion moieties, quadrupole, and model: MICROTOF II. The base peak appears at 279.20 m/z and the molecular ion peak appears at 206.1245 m/z. The molecular mass of ionic liquid was approximately 256.20 g $mole^{-1}$ depicted from the mass spectrum shown in fig. 8.

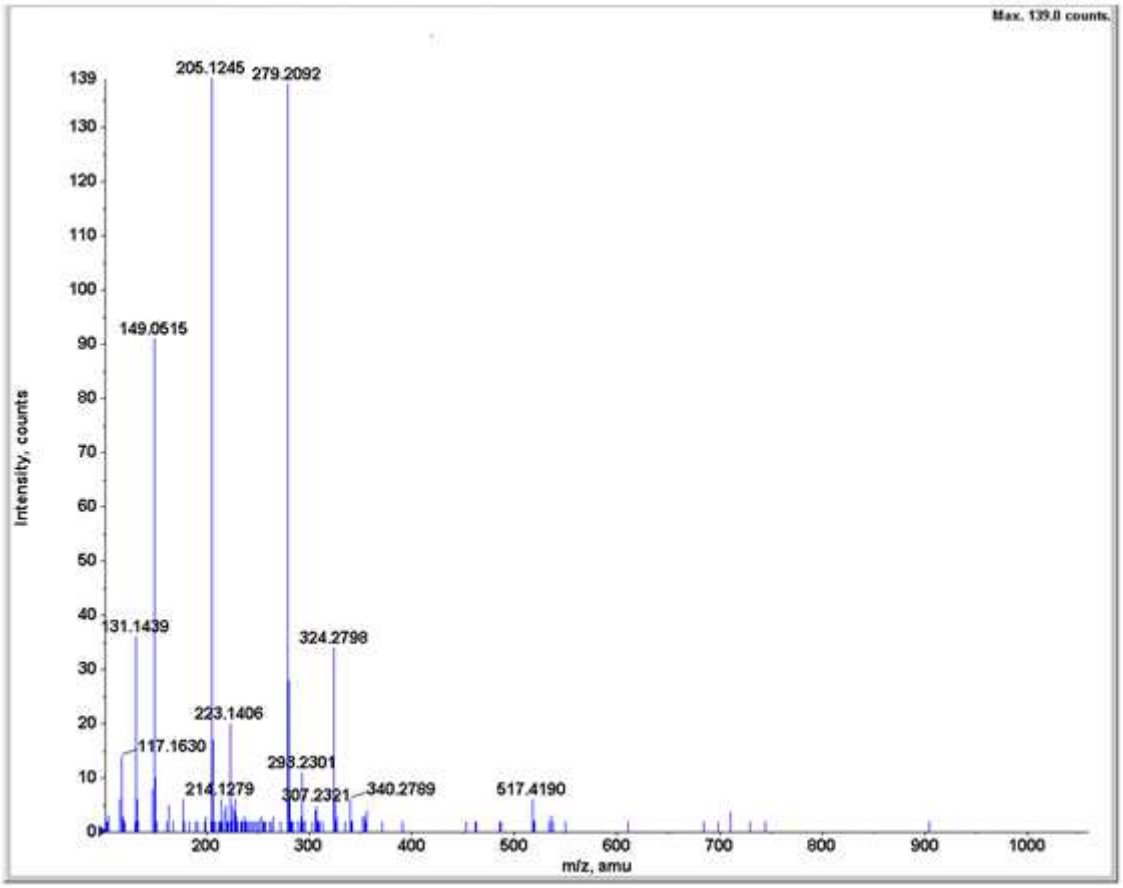

Figure 8. Mass Spectrum of synthesized ionic liquid

3.2. Saturation studies of Carbon dioxide absorption

The experimental studies of CO_2 absorption reveals that 0.7 M aqueous solution of ionic liquid can absorb up to 1.57 mole of carbon dioxide per mole of ionic liquid at ambient conditions as shown in fig. 9. There is a continuous increase in the CO_2 concentration in ionic liquid with time. After 70 hours of continuous bubbling, the solution

354 became very viscous which stops the further diffusion of CO_2 molecules in it and it showed levelling off in the
355 concentration of CO_2.

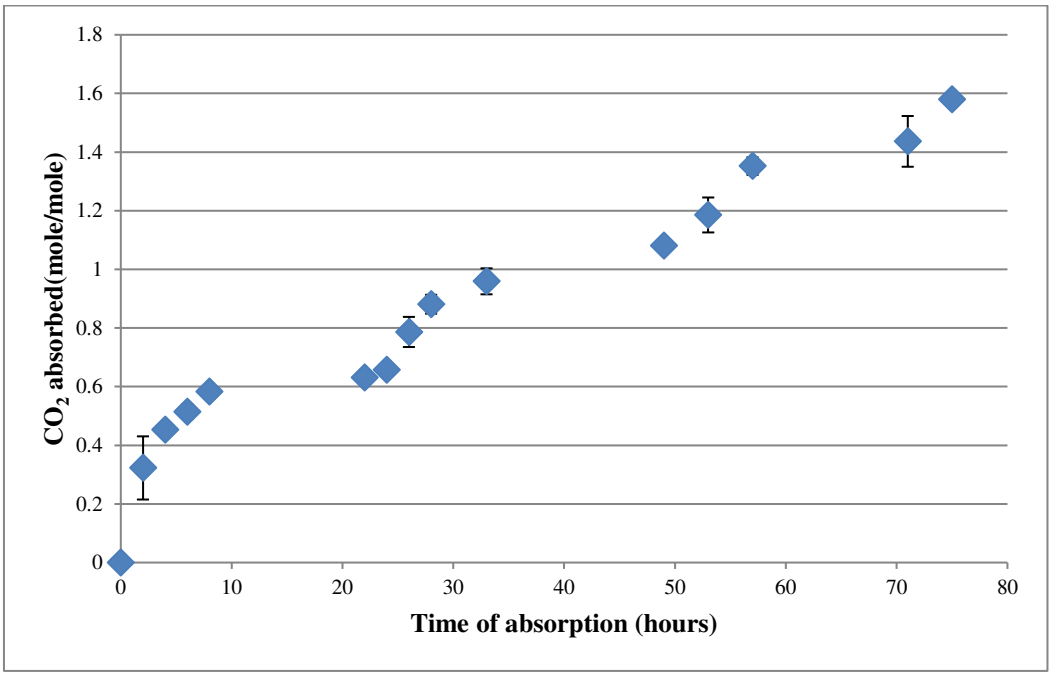

356

357 **Figure 9:** *carbon dioxide absorption in 0.7M aqueous solution of TETAL*

358 As per the literature, in the beginning of absorption the carbamate formation predominated but the end carbamate
359 is converted into bicarbonates which are water soluble. By wet chemistry test, it was confirmed as the end product
360 is ammonium bicarbonate. A lower energy is required to break the bicarbonate bond in comparison to the
361 carbamate as calculated from Gaussian 03. Thus, carbon dioxide rich ionic liquid requires less energy for
362 regeneration.

363 $$NH_4HCO_3 \Delta\leftrightarrow \ NH_3 + CO_2 + H_2O, \quad \Delta H = 15.8\ kcal/mol$$

364 $$RNHCOOH\ \Delta\leftrightarrow\ RNH_2 + CO_2, \quad \Delta H = 38.6\ kcal/mol$$

365 The kinetic studies of CO_2 absorption reaction in the synthesized ionic liquid triethylenetetrammonium lactate
366 (TETAL) were conducted at different temperatures 299, 308, 313, 323, and 333 K and initial concentrations of
367 TETAL ranged from 0.1 to 1.1 kmol m^{-3}. The effect of various factors and experimental conditions are discussed
368 in detail in this section.

3.3. Effect of different parameters on rate of CO_2 absorption

3.3.1. Viscosity

Viscosity of solvent in gas liquid absorption reactions plays a very important role in chemical kinetics. Most of the ionic liquids are highly viscous due to which the pumping cost increases (Mota-Martinez *et al.*, 2018). The viscosity of the ionic liquid affects the diffusivity of gas molecules. Therefore, the viscosity of the synthesized ionic liquid was measured as a function. The change in viscosity is very fast with increase in temperature as shown in fig. 10.

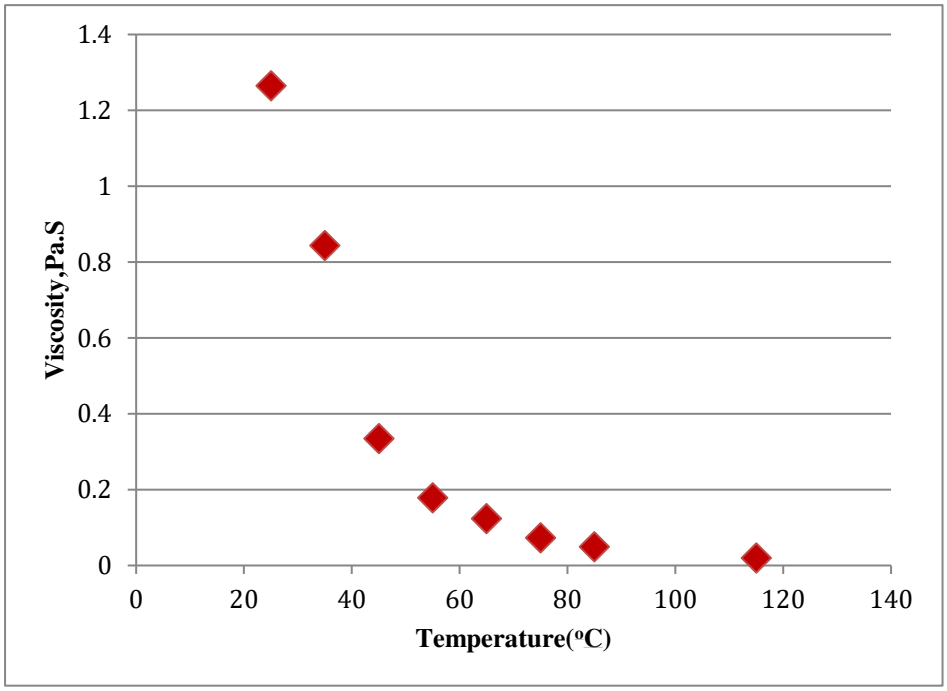

Figure 10. Variation in Viscosity of [TETA] [Lactate] with temperature

This indicates that at 308 K its viscosity is similar to water solvent. On this basis the diffusivity constant can be taken as the same for the same concentration and temperature. All the other hydrodynamic properties which play an important role in CO_2 absorption are calculated and tabulated below in table 8.

Table 8: Calculated Viscosity, Henry's constant and diffusivity data of [TETA] [Lactate] at different temperatures and different concentrations

C_{TETAL} (kmol m^{-3})	T (K)	$\mu_{aqu.TETAL}$ (× 10^{-3} Pa s)	H_{CO_2} (×10^{-4} mol m^{-3} Pa^{-1})	D_{CO_2} (×10^{-9} m^2 s^{-1})
0.1	299	1.091	2.14	1.64

	308	1.052	1.92	1.78
	313	1.001	1.75	1.92
	323	0.948	1.57	2.14
	333	0.892	1.43	2.48
	299	1.097	2.1	1.63
	308	1.064	1.9	1.77
	313	1.021	1.71	1.91
	323	1.001	1.54	2.11
	333	0.923	1.41	2.53
0.5	299	1.104	2.06	1.62
	308	1.084	1.86	1.74
	313	1.071	1.67	1.84
	323	1.050	1.51	2.06
	333	0.929	1.39	2.50
	299	1.156	2.02	1.61
	308	1.100	1.82	1.73
0.7	313	1.080	1.63	1.86
	323	1.056	1.48	2.05
	333	1.020	1.37	2.47
	299	1.117	1.98	1.61
	308	1.092	1.78	1.73
0.9	313	1.048	1.59	1.85
	323	0.942	1.45	2.15
	333	0.899	1.35	2.40
	299	1.124	1.94	1.60
	308	1.102	1.75	1.72
1.1	313	1.052	1.55	1.84
	323	0.995	1.42	2.06
	333	0.902	1.31	2.39

3.3.2. Density

The density of synthesized pure ionic liquid was measured using densitometer (Model: DE45 Mettler Toledo) with a precision of ± 0.005 kg/m^3 in the range of 283 to 363. The volume of the sample taken was 15 mL. The decrease in density is showing linear profile with respect to the increase in temperature as depicted in fig. 11. The density and viscosity of the liquid phase have the greatest impact on the packing height design as well as the absorption unit's capital cost.

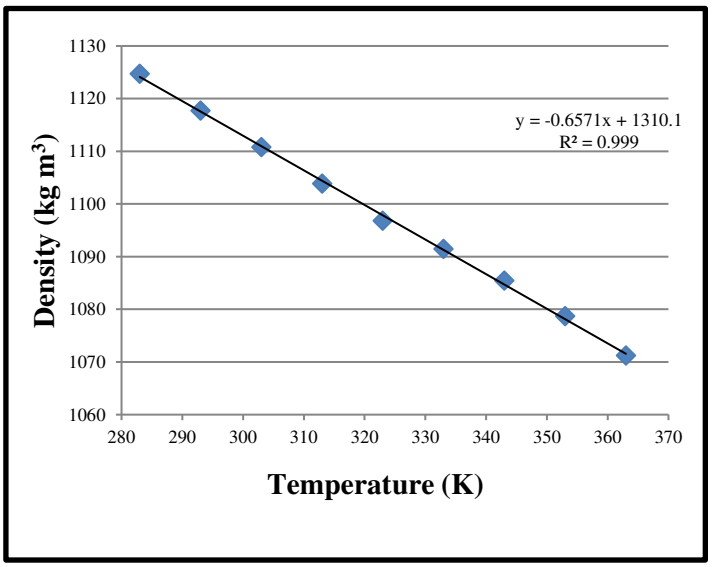

Figure 11. The behavior of Density of [TETA] [Lactate] with temperature

3.3.3. Influence of Stirring Speed

In a gas-liquid absorption reaction, the rate of gas absorption also depends on the reactor dimensions, the geometry and number of impellers, and the stirring speed. The absorption rate is directly affected by the diffusional domain for which a large interfacial area was required. In a stirred reactor, the stirring improved the diffusion of the gas into the liquid film (Contreras Moreno *et al.*, 2017). The influence of the stirring speed on the liquid side mass - transfer coefficient was investigated. The agitation speeds were kept relatively low to avoid disturbing the planar interface. The liquid-side mass - transfer coefficient can be represented as (Littel, Versteeg and Van Swaaij, 1992)

$$k_L = f(\rho, \mu, D_{CO_2}, D_s, N_L, D_{Stirred\ cell}) \qquad \ldots(22)$$

$$\frac{dC_{CO_2}}{dt} = \frac{k_l a}{V_l}\left(C^*_{CO_2} - C^{bulk}_{CO_2}\right) \qquad \ldots(23)$$

In equation (22), k_L $(liquid\ side\ mass\ transfer\ coefficient)$ is a function of ρ, density of absorbing solution, μ, viscosity of absorbing solution, D_{CO_2}, diffusivity of CO_2 in the absorbing solution, D_s, the diameter of impeller blades in the liquid-phase, N_L, Stirring rate in liquid phase, $D_{Stirred\ cell}$, the inner diameter of a stirred tank reactor.

It was noticed that the measured $k_L a$ increased on increasing the stirring speed up to certain extent and then it remained constant. This is due to the decrease in the liquid film thickness δ responsible for the resistance to the mass - transfer of carbon - dioxide gas molecules. From the experimental measurements shown in the Fig. 12, it is observed that the rate of CO_2 absorption appear practically constant between 60-80 rpm. In this range, values of volumetric mass transfer coefficient is same ($k_L a$) (fig. 13), therefore the reaction is in the kinetic regime at this stirring speed.

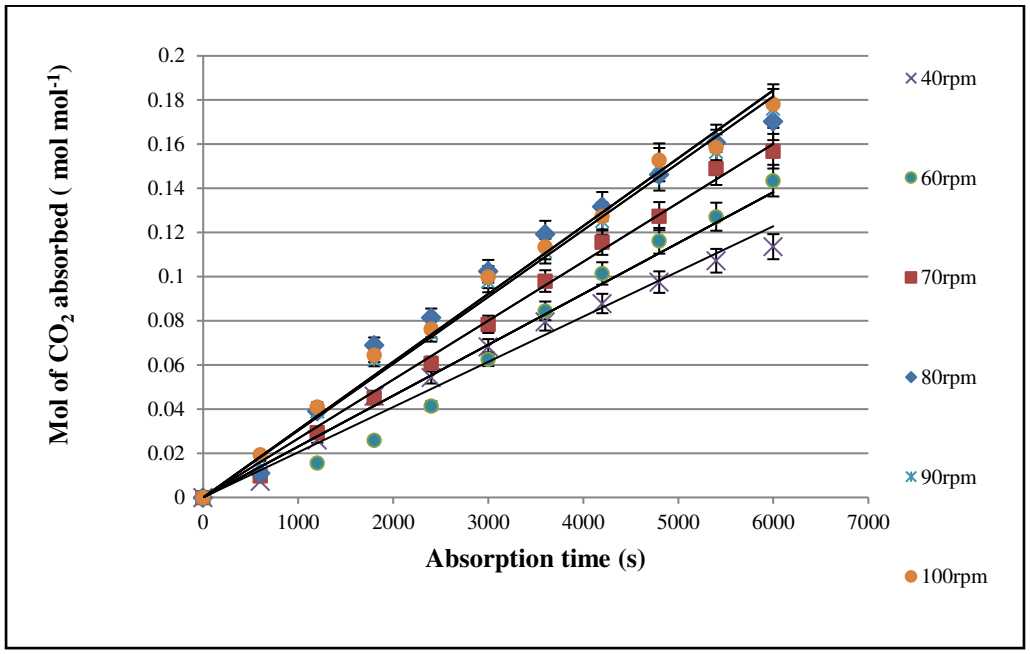

Figure 12. Effect of stirring speed on CO_2-absorption rate in 0.1 kmol/m^3ionic liquid solution at 299K and 101.325 kPa

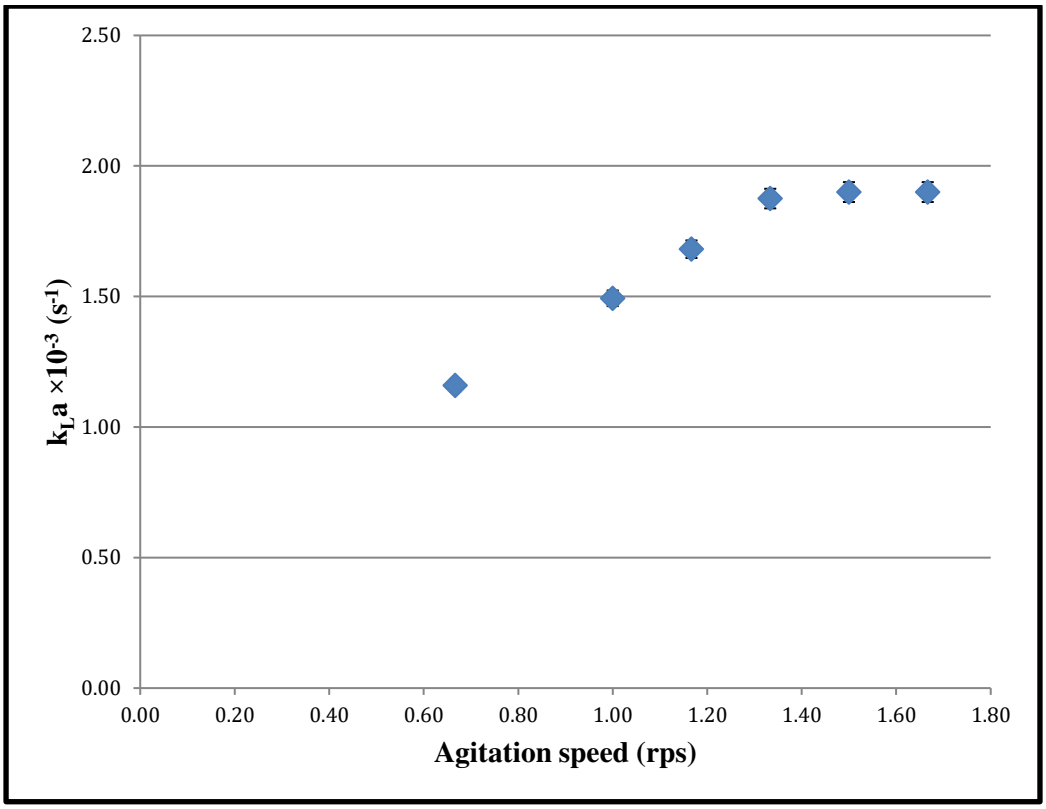

Figure 13. Volumetric Mass-transfer Coefficient of CO_2 at different Stirring Speeds

3.3.4. Effect of Initial Concentration of Ionic Liquid and Partial Pressure of CO2 gas

In this study, the pure carbon-dioxide gas was bubbled in different initial concentrations of ionic liquid at 308 K and 101,325 kPa at a flow rate of 2.83×10^{-5} m^3 s^{-1}. The rate of CO_2 absorption was also determined with respect to the different partial pressure of CO_2 gas by pressure dropping method. As per the studies, on increasing the concentration of ionic liquid, the carbon - dioxide uptake increases up to a certain limit and then becomes constant. During CO_2 absorption, the solution temperature also increased by ± 5°C due to an exothermic process but try to maintain it using a double jacket filled with circulated water. From the experimental data, the rate constant at different concentrations of ionic liquid is calculated using the equation is tabulated in table 9. It is also observed that with CO_2 uptake, the viscosity of the absorbing solution also increases, which in turn decreases the diffusivity of further CO_2 gas and thus the rate becomes constant after some time.

The experimental data is plotted in fig. 14.

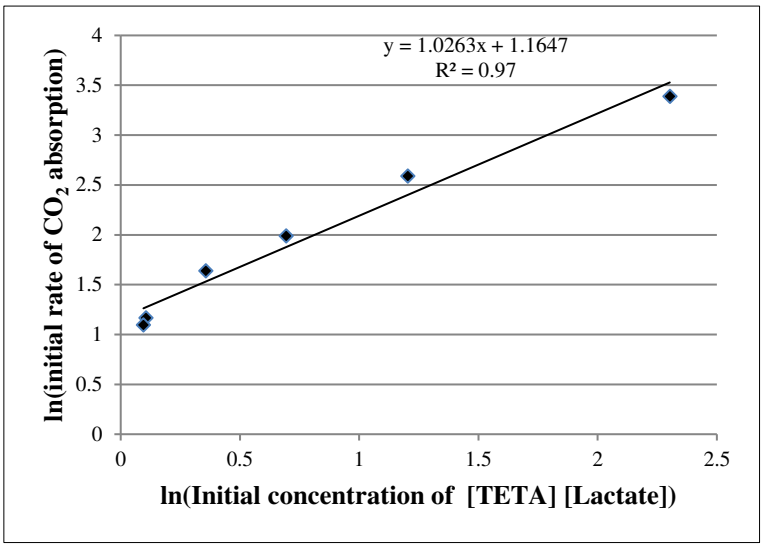

425

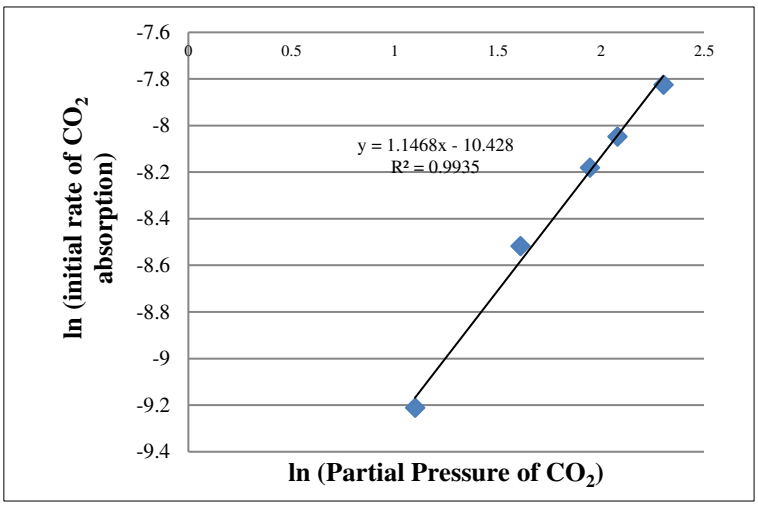

426

427

428 Figure 14. Effect of initial concentration of [TETA] [Lactate] and partial pressure of carbon dioxide on the rate
429 of absorption (T = 308 K, P = 101.325 kPa, stirring rate in liquid phase, N_L = 80 rpm, stirring rate in gas-phase,
430 N_G = 120 rpm.

431

432 **Table 9:** Calculated value of rate constant of pseudo first order reaction at T = 308 K and P = 101.325 kP

C_{TETAL} (kmol m^{-3})	k_2 (Experimental) (× 10^3 m^3 mol^{-1} s^{-1})
0.1	1.27
0.3	1.47
0.5	1.67
0.7	1.88
0.9	2.08

1.1	2.30

The reaction rate for the studied chemical absorption reaction is found to be first order with respect to both initial concentration of [TETA] [Lactate]and partial pressure of CO_2 which is in the good agreement of the available literature (Yuan and Rochelle, 2018) (Blauwhoff, Versteeg and Van Swaaij, 1984).

3.3.5. Effect of Temperature on Absorption

The effect of temperature has also been tested on the rate of CO_2 absorption. As per the theory, the rate of reaction doubles at every 10 °C increment in temperature. Initially, with an increase in the temperature, the rate of absorption of CO_2 gas increases as shown in Fig. 15. At different temperature, the second-order reaction rate constant, k_2, can be calculated using the Arrhenius expression (Jamal, Meisen and Jim Lim, 2006)

$$k_2 = A.e^{\frac{-E_a}{RT}} \quad \ldots(24)$$

Here, A is the Arrhenius constant or pre-exponential constant (m^3 mol s^{-1}), Ea represents the activation energy (kJ mol^{-1}), and R represents the universal gas constant (0.008315 kJ mol^{-1} K^{-1})

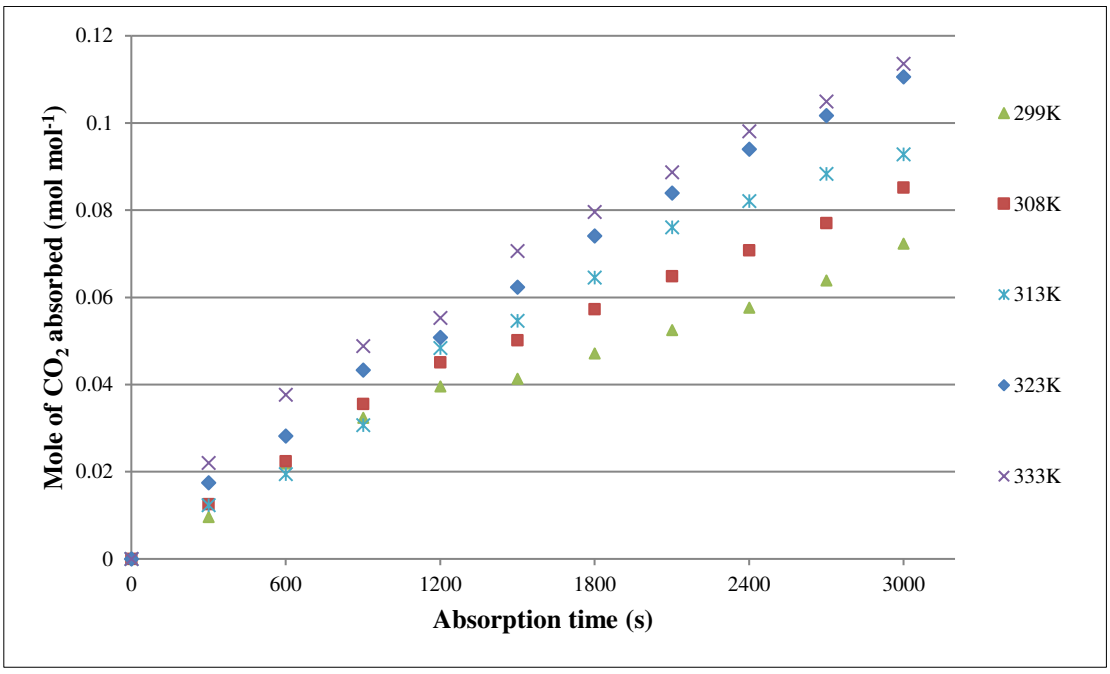

(a)

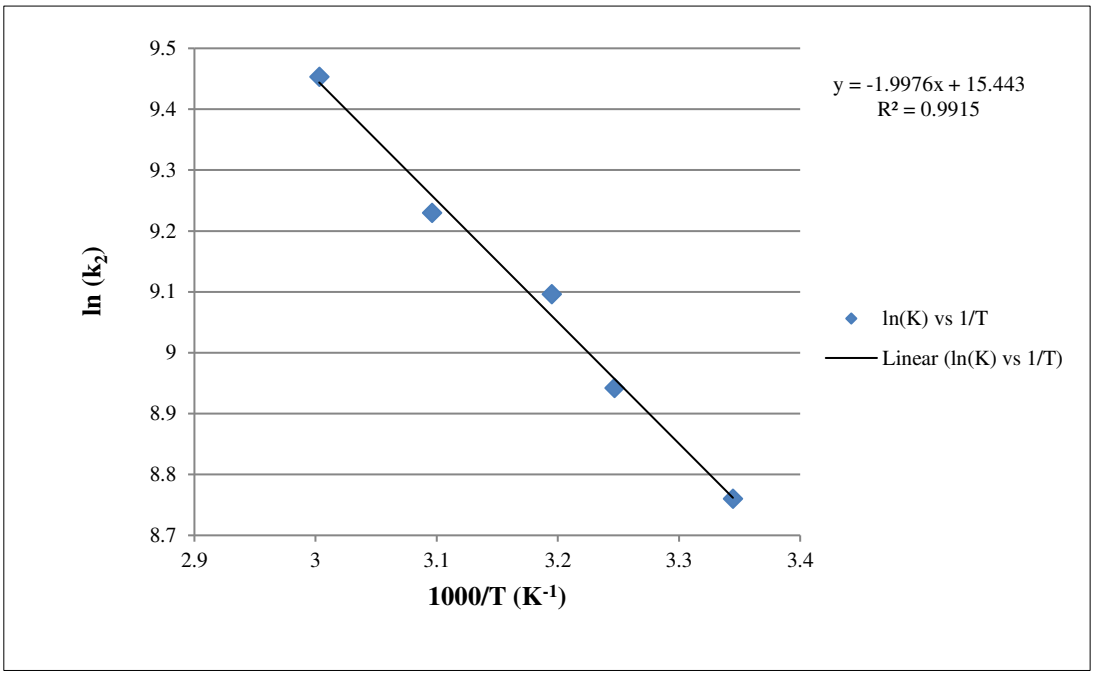

(b)

Figure 15. (a) The rate of CO_2-absorption at different temperature in 0.1 kmol m^{-3} of [TETA] [Lactate] solution (b) Arrhenius plot for CO_2-absorption reaction in [TETA] [Lactate] solution

The plot of $ln\ k_2$ versus 1000/T, leads from the Arrhenius expression for the kinetic constant

$$ln\ ln\ k_2 = ln\ ln\ A - \frac{E_a}{RT} \quad \ldots(25)$$

From the graph,

$$ln\ ln\ k_2 = 15.443 - 1.9976\left(\frac{1000}{T}\right) \quad \ldots(26)$$

$$k_2 = 5.09 \times 10^6 exp\left(-\frac{1997.6}{T}\right) \quad \ldots(27)$$

The second order reaction rate constants follow Arrhenius behavior with the activation energy of 16.61 kJ mol^{-1} measured for [TETA][Lactate] which is in good agreement with similar ILs (Gurkan *et al.*, 2013). Table 10, shows the calculated values of second order rate constant for CO_2 absorption at various temperatures.

Table 10. Calculated values of second-order rate constant from Arrhenius plot

Temperature (K)	**k_2 (m^3 mol^{-1} s^{-1})**
299	6385.93
308	7762.61

313	8610.00
323	10490.95
333	12632.01

The overall reaction rate expression for CO_2-absorption is therefore deduced as:

$$R_{CO_2} = 9.48 \times 10^3 m^3 mol^{-1} s^{-1}. C_{TETAL}^{1.026}. C_{CO_2}^{1.146} \quad \ldots (28)$$

As, $1.026 \approx 1$ and $1.146 \approx 1$,

$$R_{CO_2} = 9.48 \times 10^3 m^3 mol^{-1} s^{-1}. C_{TETAL}. C_{CO_2} \quad \ldots (29)$$

4. Observations and Conclusion

This technique of transformation proved to be better for CO_2 absorption at high temperature. In this work we have reported the absorption capacity of synthesized ionic liquid and the effect of physicochemical properties on CO_2 absorption rate. The synthesized protic ionic liquid is easy to synthesize and also a low-cost ionic liquid. The carbon dioxide absorption capacity in aqueous solution of ionic liquid reached up to 1.57 mole of carbon dioxide absorbed /mole of ionic liquid. This represents the very good absorption capacity to cost ratio in comparison with the benchmarked solvent, MEA (0.55 mol of CO_2/mol of amine). The kinetic regime of carbon-dioxide absorption corresponds to a fast pseudo-first-order reaction for the controlled conditions employed in this research. The second order reaction rate constants follow Arrhenius behavior with the activation energy of 16.61 kJ mol^{-1} measured for [TETA] [Lactate]. The ILs studied in this work exhibit reactivity comparable to or higher than commonly used ammonium based IL. In aqueous [TETA] [Lactate] solution, the pseudo first-order rate constant at different temperatures for the CO_2-absorption reaction was found to be 9.48×10^3 m^3 mol^{-1} s^{-1}. The physical properties like viscosity, diffusivity, and density of ionic liquid played a significant role in the rate of reaction kinetics. At last, the authors conclude the statement that transformation of amines into ionic liquid could be the benchmark solvent for carbon dioxide absorption in future.

Ethics approval and consent to participate

N/A

Consent for Publication

N/A

Availability of data and materials

All data generated or analysed during this study are included in this published article.

Declaration of Competing Interest

The authors declared that there is no conflict of interest.

Funding

Amita Chaudhary reports financial support, equipment, drugs, or supplies from CSIR-UGC Delhi as a Junior Research Fellowship and Senior research Fellowship. She get the administrative support, writing assistance from Chemical Engineering Department, Indian Institute of Technology Delhi.

Authors contributions

Amita Chaudhary: Experiments, Conceptualization, Writing - original draft, Data collection and compilation, manuscript processing.

Ashok N Bhaskarwar: Revising original draft of manuscript and technical guidance.

Acknowledgments

The authors are grateful to CSIR-UGC, Delhi, for providing financial support to one of us for conducting this research work. We would also like to acknowledge the Indian Institute of Technology, Delhi, India, for facilitating us with the research facilities for the completion of this research work.

References

Ahmady, A., Hashim, M. A. and Aroua, M. K. (2012) 'Kinetics of Carbon Dioxide absorption into aqueous MDEA+[bmim][BF4] solutions from 303 to 333K', *Chemical Engineering Journal*, 200–202, pp. 317–328. doi: https://doi.org/10.1016/j.cej.2012.06.037.

Blauwhoff, P. M. M., Versteeg, G. F. and Van Swaaij, W. P. M. (1984) 'A study on the reaction between CO2 and alkanolamines in aqueous solutions', *Chemical Engineering Science*, 39(2), pp. 207–225. doi: https://doi.org/10.1016/0009-2509(84)80021-4.

Caplow, M. (1968) 'Kinetics of carbamate formation and breakdown', *Journal of the American Chemical Society*. American Chemical Society, 90(24), pp. 6795–6803. doi: 10.1021/ja01026a041.

Chaudhari, R.V., and L.K. Doraiswamy. 1974. "Absorption of Phosphine in an Aqueous Solution of

512 Formaldehyde and Hydrochloric Acid." Chemical Engineering Science 29: 129–33.

513 Chen, Y. *et al.* (2020) 'Capture of Toxic Gases by Deep Eutectic Solvents', *ACS Sustainable Chemistry &*
514 *Engineering*. American Chemical Society, 8(14), pp. 5410–5430. doi: 10.1021/acssuschemeng.0c01493.

515 Contreras Moreno, V. *et al.* (2017) 'Valorisation of CO2 with epoxides: Influence of gas/liquid mass transfer on
516 reaction kinetics', *Chemical Engineering Science*, 170, pp. 77–90. doi: https://doi.org/10.1016/j.ces.2017.01.050.

517 Crossno, S. K., Kalbus, L. H. and Kalbus, G. E. (1996) 'Determinations of Carbon Dioxide by Titration: New
518 Experiments for General, Physical, and Quantitative Analysis Courses', *Journal of Chemical Education*.
519 American Chemical Society, 73(2), p. 175. doi: 10.1021/ed073p175.

520 Danckwerts, P. V (1979) 'The reaction of CO2 with ethanolamines', *Chemical Engineering Science*, 34(4), pp.
521 443–446. doi: https://doi.org/10.1016/0009-2509(79)85087-3.

522 Gates, B. C. 1985. "Heterogeneous Reactions: Analysis, Examples, and Reactor Design. by L. K. Doraiswamy
523 and M. M. Sharma, John Wiley and Sons, 1984, Volume 1: Gas-Solid and Solid-Solid Reactions, 538 Pp.,$66.95;
524 Volume 2: Fluid-Fluid-Solid Reactions, 374 Pp.,$59.95." AIChE Journal 31 (8): 1405–1405.
525 https://doi.org/10.1002/aic.690310822.

526 Gupta, R. K., and M. M Sharma. 1967. "Absorption of Carbon Dioxide and Chlorine in Aqueous Solutions of
527 Barium Sulfide." Indian Chem. Eng. Trans, 100–106.

528 Gurkan, B. E. *et al.* (2013) 'Reaction kinetics of CO2 absorption in to phosphonium based anion-functionalized
529 ionic liquids', *Physical Chemistry Chemical Physics*, 15(20), p. 7796. doi: 10.1039/c3cp51289d.

530 Jamal, A., Meisen, A. and Jim Lim, C. (2006) 'Kinetics of carbon dioxide absorption and desorption in aqueous
531 alkanolamine solutions using a novel hemispherical contactor—I. Experimental apparatus and mathematical
532 modeling', *Chemical Engineering Science*, 61(19), pp. 6571–6589. doi:
533 https://doi.org/10.1016/j.ces.2006.04.046.

534 Jean-Mare, G., Amann, and C Bouallou. 2009. "Kinetics of the Absorption of CO2 in Aqueous Solutions of N-
535 Methyldiethanolamine and Triethylene Tetramine." Ind. Eng. Chem. Res. 48: 3761–70.

536 Kucka, L., J. Richter, E. Y. Kenig, and A. Górak. 2003. "Determination of Gas/Liquid Reaction Kinetics with a
537 Stirred Cell Reactor." Separation and Purification Technology 31: 163–75.

Lee, S. *et al.* (2007) *Kinetics of CO2 Absorption in Aqueous Sodium Glycinate Solutions*, *Industrial & Engineering Chemistry Research*. doi: 10.1021/ie061270e.

Levenspiel, O. (1999) 'Chemical Reaction Engineering', *Industrial & Engineering Chemistry Research*. American Chemical Society, 38(11), pp. 4140–4143. doi: 10.1021/ie990488g.

Li, H. *et al.* (2019) 'Prediction of CO2 absorption by physical solvents using a chemoinformatics-based machine learning model', *Environmental Chemistry Letters*, 17(3), pp. 1397–1404. doi: 10.1007/s10311-019-00874-0.

LITTEL, R., VERSTEEG, G. and VAN SWAAIJ, W. (1992) 'Kinetics of CO2 with primary and secondary amines in aqueous solutions-I-Zwitter deprotonation kinetics for DEA and DIPA in aqueous blends of alkanolamines', *Chemical Engineering Science*, 47(8), pp. 2027–2035.

Liu, S. *et al.* (2018) 'High CO2 adsorption by amino-modified bio-spherical cellulose nanofibres aerogels', *Environmental Chemistry Letters*, 16(2), pp. 605–614. doi: 10.1007/s10311-017-0701-8.

Lu, B. *et al.* (2013) 'Kinetics of Carbon Dioxide Absorption into Mixed Aqueous Solutions of MEA + [Bmim]BF4 Using a Double Stirred Cell', *Energy & Fuels*. American Chemical Society, 27(10), pp. 6002–6009. doi: 10.1021/ef400976j.

Lahiri, R. N., G. D. Yadav, and M. M. Sharma. 1981. "Absorption of Chlorine in Aqueous Solutions of Sodium Hydroxide: Desorption of Hypochlorous Acid Followed by Its Dissociation to Chlorine Monoxide." Chemical Engineering Science 38: 1119–33.

Linek, V. 1966. "Rate of Absorption of Oxygen into a Sulphite Solution in the Presence of a Copper or Cobalt Catalyst Using a Mechanical Agitator." Chemical Engineering Science 21: 777–90.

Miller, S.A. 1969. "Ethylene and Its Industrial Derivatives." In Ernest Benn, London, 658.

Mondal, B. K. and Samanta, A. N. (2020) 'Equilibrium solubility and kinetics of CO2 absorption in hexamethylenediamine activated aqueous sodium glycinate solvent', *Chemical Engineering Journal*, 386, p. 121462. doi: https://doi.org/10.1016/j.cej.2019.04.042.

Mota-Martinez, M. T. *et al.* (2018) 'Challenges and opportunities for the utilisation of ionic liquids as solvents for CO2 capture', *Molecular Systems Design & Engineering*. The Royal Society of Chemistry, 3(3), pp. 560–571. doi: 10.1039/C8ME00009C.

564 Mukherjee, S., Bandyopadhyay, S. S. and Samanta, A. N. (2018) 'Kinetic Study of CO2 Absorption in Aqueous
565 Benzylamine Solvent Using a Stirred Cell Reaction Calorimeter', *Energy & Fuels*. American Chemical Society,
566 32(3), pp. 3668–3680. doi: 10.1021/acs.energyfuels.7b03743.

567 Oyevaar, MH, and KR Westerterp. 1989. "The Use of the Chemical Method for the Determination of Interfacial
568 Areas in Gas-Liquid Contactors." Chemical Engineering Science 44 (11): 2691–2701.

569 Sander, R. (2015) 'Compilation of Henry's law constants (version 4.0) for water as solvent', *Atmos. Chem. Phys.*
570 Copernicus Publications, 15(8), pp. 4399–4981. doi: 10.5194/acp-15-4399-2015.

571 Sun, C. *et al.* (2017) 'Mechanism and Kinetics Study of CO2 Absorption into Blends of N-Methyldiethanolamine
572 and 1-Hydroxyethyl-3-methylimidazolium Glycine Aqueous Solution', *Energy & Fuels*. American Chemical
573 Society, 31(11), pp. 12425–12433. doi: 10.1021/acs.energyfuels.7b01942.

574 Sauchel, V. 1960. "No Title." Chemistry and Technology of Fertilizers, Reinhold, New York, 10.

575 Sharma, M. M. 1964. "Kinetics of Gas Absorption." Ph.D Thesis, Cambridge University, England.

576 Stevanovic, S., A. Podgorsek, L. Moura, C. C. Santini, A. A H Padua, and M. F. Costa Gomes. 2013. "Absorption
577 of Carbon Dioxide by Ionic Liquids with Carboxylate Anions." International Journal of Greenhouse Gas Control.
578 https://doi.org/10.1016/j.ijggc.2013.04.017.

579 Thummuru, D. N. R. and Mallik, B. S. (2017) 'Structure and Dynamics of Hydroxyl-Functionalized Protic
580 Ammonium Carboxylate Ionic Liquids', *The Journal of Physical Chemistry A*. American Chemical Society,
581 121(42), pp. 8097–8107. doi: 10.1021/acs.jpca.7b05995.

582 Versteeg, G. F. and Van Swaaij, W. P. M. (1988) 'Solubility and diffusivity of acid gases (carbon dioxide, nitrous
583 oxide) in aqueous alkanolamine solutions', *Journal of Chemical & Engineering Data*. American Chemical
584 Society, 33(1), pp. 29–34. doi: 10.1021/je00051a011.

585 Ying, J., and D. A Eimer. 2013. "Determination and Measurements of Mass Transfer Kinetics of CO2 in
586 Concentrated Aqueous Monoethanolamine Solutions by a Stirred Cell." Ind. Eng. Chem. Res. 52: 235–243.

587 Yuan, Y. and Rochelle, G. T. (2018) 'CO2 absorption rate in semi-aqueous monoethanolamine', *Chemical*
588 *Engineering Science*, 182, pp. 56–66. doi: https://doi.org/10.1016/j.ces.2018.02.026.

589 Zhang, Xin *et al.* (2014) 'Gas–liquid mass-transfer properties in CO2 absorption system with ionic liquids', *AIChE*

590 *Journal*. John Wiley & Sons, Ltd, 60(8), pp. 2929–2939. doi: 10.1002/aic.14507.

591 Zhou, J. M., Jing, G. H. and Zhou, L. J. (2012) 'Characterization and absorption of carbon dioxide into aqueous
592 solution of amino acid ionic liquid [N1111][Gly] and 2-amino-2-methyl-1-propanol.', *Chemical Engineering*
593 *Journal*, 204, pp. 235–243.

594 Zhou, Z. *et al.* (2016) 'Performance and reaction kinetics of CO2 absorption into AMP solution with [Hmim][Gly]
595 activator', *International Journal of Greenhouse Gas Control*, 44, pp. 115–123. doi: 10.1016/j.ijggc.2015.11.010.